Results in Engineering 15 (2022) 100448

Contents lists available at ScienceDirect

Results in Engineering

journal homepage: www.sciencedirect.com/journal/results-in-engineering

# Effects of thermophoresis and Brownian motion for thermal and chemically reacting Casson nanofluid flow over a linearly stretching sheet

Jagadish V. Tawade [a], C.N. Guled [b], Samad Noeiaghdam [c,d,*], Unai Fernandez-Gamiz [e], Vediyappan Govindan [f], Sundarappan Balamuralitharan [g]

[a] Department of Mathematics, Vishwakarma University, Kondhwa(BK), Pune, 411048, Maharashtra, India
[b] Department of Applied Sciences, Indian Institute of Information Technology, Pune, 411048, Maharashtra, India
[c] Industrial Mathematics Laboratory, Baikal School of BRICS, Irkutsk National Research Technical University, Irkutsk, 664074, Russia
[d] Department of Applied Mathematics and Programming, South Ural State University, Lenin prospect 76, Chelyabinsk, 454080, Russia
[e] Nuclear Engineering and Fluid Mechanics Department, University of the Basque Country UPV/EHU, Nieves Cano 12, 01006, Vitoria-Gasteiz, Spain
[f] Department of Mathematics, DMI St John the Baptist University, Mangochi, 409, Central Africa, Malawi
[g] Department of Mathematics, Bharath Institute of Higher Education and Research, Selaiyur, Chennai, 600 073, Tamil Nadu, India

ARTICLE INFO

*Keywords:*
Linear stretching sheet
Similarity transformation
Heat transfer
Thermophoresis
Brownian motion
Casson nanofluid

ABSTRACT

The current research explores the problem of steady laminar flow of nanofluid on a two dimensional boundary layer using heat transfer of Cassona cross the linearly stretching sheet. The governing equations are partial differential equations which are transformed into non-linear ordinary differential equations by using some similarity transformation. The converted form of the combined non-linear higher-order ODEswith a set of boundary conditions are solved by means of Runge-Kutta 4th-order approach along with the shooting method. The nanoparticle concentration profiles, velocity, and temperature are examined by taking account of their influence of Prandtl number, "Brownian motion parameter", Lewis number, thermophoresis, and Casson fluid parameter. It is reported that the temperature increase as Nt and Nb increases which causes thickening of the thermal boundary layer. Also it is observed that, there is increment in temperature profile for increasing values of Brownian motion parameter and the energy distribution grows with increment in the values of Thermophoresis parameter. The comparison for the local Nusselt & local Sherwood number has been tabulated with respect to variation of the Brownian Motion Parameter and Thermophoresis parameter. All the findings of the results are graphically represented and discussed.

## 1. Introduction

The research on boundary layer flow along with heat transfer across the linearly stretched plate was quite successful over the past few years because of their broad variety of usages in science and industry. A few of these uses are materials produced via metal spinning, metal extrusion, glass fibre, wire drawing, hot rolling, artificial fibres, continuous stretching of the plastic films, drawing of copper wires, and polymer extrusion, etc. The current study focuses on the boundary layer flows, heat transfer with chemical reaction of Casson nano fluids across a stretching surface. The liquid which flows is called fluid. A nano fluid has a base fluid which has several nanoparticles. Nano particles are the particles whose diameter ranges from 1 to 100 nm. The base fluid is like water ethylene, glycol, and toluene. Then carbides, metals, oxides or non-metals are added to base fluid then the fluid becomes nano fluid. The aim of taking nano fluids is to study about the thermal properties of the liquid. The thermal conductivity of nano fluids can be doubled by adding nanoparticles to the base fluid. This type of increase in thermal conductivity is used in cooling heat exchanges, double plane windows etc.

The heat transmission characteristics are an essential element as per the boundary layer flow of a "Casson nanofluid" across a stretching plate. The properties of heat transfer across a stretching plate are significant to understand in order to achieve the required quality. This is due to the value of the finished product relies primarily on stretching rate and heat transfer rate.

* Corresponding author. Industrial Mathematics Laboratory, Baikal School of BRICS, Irkutsk National Research Technical University, Irkutsk, 664074, Russia.;
*E-mail addresses:* jagadish.tawade@vupune.ac.in (J.V. Tawade), Guledcom89@gmail.com (C.N. Guled), snoei@istu.edu, noiagdams@susu.ru (S. Noeiaghdam), unai.fernandez@ehu.eus (U. Fernandez-Gamiz), govindoviya@gmail.com (V. Govindan), balamuralitharan.maths@bharathuniv.ac.in (S. Balamuralitharan).

https://doi.org/10.1016/j.rineng.2022.100448
Received 4 April 2022; Received in revised form 10 May 2022; Accepted 12 May 2022
Available online 24 May 2022

Following a pioneering study by Sakiad is [1] boundary fluid layer flow of "Newtonian", as well as "non-Newtonian" fluids across the non-1inear or 1inear stretching plate, contains a broad range of literature. Moreover, many scholars studied the different features of heat transfer and boundary layer flow issues thoroughly across linear/nonlinear stretching sheets (see Refs. [2–10]). Nieldand Kuznestov [11] have investigated the normal convective nanofluid flow on a boundary layer across a vertical sheet. They utilized a paradigm that considered Brownian motion as well as thermophoresis impact. Shanker and Ibrahim [12] investigated the boundary-layer flow & nanofluid heat transfer across a vertical sheet considering the boundary condition for convective surface. Moreover, Aziz and Makinde [13] have performed a numerical analysis of a nanof1uid flow on the boundary layer through a stretching plate with a set of boundary conditions. Mustafa et al. [14] recommended the nano-fluid flow at a stagnation point across a stretching plate. Pop & Khan [15] have assessed the nanofluid's flow on a boundary layer with a steady surface temperature across a stretching surface. For more studies on nanofluid see Refs. [16–19].

Lately, Mohammad Ghalambaz, Rashid Pourrajab, and Aminreza Noghrehabadi [20], have examined the impact of partial slip conditions across a nanofluids flow & heat transfer through stretching sheet, with proposed temperature on the constant wall. This issue is addressed by utilizing the shooting approach with the "Runge-Kutta-Fehlberg" method. They showed that the decreased Sherwood, as well as Nusselt numbers, are significantly affected by the slip speed variable. Bandari Shankar and Wubshet Ibrahim [21], reviewed the heat transfer along with the flow of the boundary layer across a stretching plate considering a nanofluid under the impact of the magnetic field, thermal radiation, and set of boundary conditions. Magyari and Keller [22] appeared to be the first to examine the heat transfer and flow of boundary layers across exponentially stretching sheets.

Nazar and Bidin [23], Ishak [24], and Nadeem et al. [25,26] investigated flow along with heat transfer across thermal radiation exponentially stretching surface in numerical terms. Elbashbeshy [27] investigated the flow & heat transmission numerically across an increasingly stretching surface including suction of wall mass. Sanjayan and Khan [28] reported the flow as well as heat transfer of the viscoelastic boundary layer owing to the stretching plate. AnuarIshak [24] explored the Magneto hydrodynamic flow on boundary layer owing to the exponentially permeable stretching plate along with radiation impact. Shweta Agarwal, V. Singh [29] used an exponentially stretching surface with thermal conductance and radiation in permeable media to examine the effect of thermal transfer for 2 types of viscoelastic fluids. S. Nadeem et al. [30], & N. S. Akbar et al. [31], explored the nanofluid flow of Casson across a stretching plate.

Rabbi [34] Controlling the drift of nanofluid requires a computational technique for mass and heat transfer enhancement/reduction. On the slanted stretched surface, the fluid is dripping. This numerical research necessitates the solution of basic (conservation momentum, mass transfer, and energy) equations, which requires a high level of computational ability. Transient mixed convective laminar nanofluid flow is based on time-dependent concentration and temperature on the periphery, as well as stretched velocity. A similar transformation approach is used to convert a system of non-linear basic equations dominated by time into a differential equation of the ordinary system.

Rabbi [35] Bioengineers and medical scientists are interested in blood flow identification via the circulatory system because blood flow patterns are used in the diagnosis of circulatory illnesses such as arteriosclerotic disease. Non-Newtonian fluid models (e.g., hyperbolic tangent fluid, Powell Erying fluid, Casson fluid, Williamson fluid, etc.) were employed to assess blood flow in the cardiovascular system because these fluids give a rheological description of blood with a more detailed thinning component. Blood is used as Williamson's fluid in this experiment, and flow velocity is unstable towards the stretching/shrinking surface, in accordance with exothermic/endothermic function. The gyrotactic microorganisms (GM) hypothesis is used to nanofluid in order to stabilise nanoparticles owing to bioconvection.

Rana [36] The physical characteristics of a binary chemical reaction (BCR) and Arrhenius activation energy (ACE) on magnetohydrodynamics Williamson micropolar nanofluid flow via a vertical stretching sheet have been predicted using a mathematical framework. Temperature-dependent fluid viscosity, electrical, and thermal conductivity are assumed. Furthermore, the Lorentz force is applied at an angle to the fluid flow's normal. The non-dimensional regular expressions of the model were determined via natural transformations. Rana [37] this research looks at the effects of heat and radiation absorption on an unsteady natural convective and higher order chemically reactive magnetohydrodynamics (MHD) fluid flow. A vertical oscillating porous plate is used to create the flow. To create a flow model that captures the time-dependent momentum, energy, and diffusion balance equations, boundary layer approximations are used.

Rabbi [38] The goal of this study is to define a Casson type of Non-Newtonian fluid flow towards a stretched surface with thermophoresis and radiation absorption impacts in conjunction with a periodic hydromagnetic effect. Heat absorption is combined with the heat absorbent parameter in this case. To explain the fluid flow system, a time-dependent fundamental set of equations, including momentum, energy, and concentration, has been created.

Khan [39] this research communication's main goal is to investigate the combined effects of Ohmic heating, radiative heat flux, and viscous dissipation on the entropy-optimized reactive flow of non-Newtonian fluid toward a stretched surface. The fluid flow is generated by stretching phenomenon and is electrically conducted in the presence of an applied magnetic field. In the mathematical modelling of energy expression, the effects of heat generation/absorption, radiative heat flux, dissipation, and Ohmic heating are used. The chemical reaction is also taken into account. The total entropy rate of the Carreau–Yasuda fluid is computed using the second law of thermodynamics and compared to four irreversibilities: heat transfer irreversibility, fluid friction irreversibility, magnetic or Ohmic heating irreversibility, and chemical reaction irreversibility.

Yuming [40] The nonlinear thermal radiation and heat absorption/generation features in rate type nanofluid including gyrotactic microorganism are investigated in this communication. The flow was induced by the bidirectional periodically moving surface. Chu [41] MHD time dependent stagnation point flow of non-Newtonian fluid (Carreau fluid) is addressed in this research report while the sheet surface is stretchy and decreasing. Stagnation point flow is taken into account. The modelling of energy expression takes into consideration the innovative aspects of slip processes such as Brownian and thermophoresis diffusions.

Khan [42] the interfacial layer and shape effects for the Darcy Forchheimer electromagnetic flow of single-walled carbon nanotubes (SWCNTs) and multi-walled carbon nanotubes (MWCNTs) with base fluid (water) nanofluids were investigated computationally in this study. Nonlinear thermal radiation, as well as homogeneous and heterogeneous chemical processes, are all considered. The interfacial layer and shape impacts of carbon nanotubes-water nanofluid are measured using a revised Hamilton Crosser model. Khan [43] The Marangoni convection of hybrid nanofluid is discussed in this communication. Two nanoparticles (MnZiFe2O4–NiZnFe2O4) and one base fluid make up hybrid nanofluid (H2O). The porous media effect of Darcy Forchheimer is included in the momentum equation. Heat transfer irreversibility, mass transfer irreversibility, and viscous dissipation irreversibility generate entropy in the flow, which is measured and compared to relevant parameters.

Chu [44] the current research looks at thermal radiation qualities, heat production, and the influence of convective boundary conditions in a duct with the Rabinowitsch fluid. The thermal conductivity is a function of temperature as well. The symbolic programme Maple is used to provide the exact solution of the velocity distribution. The accurate solution of energy Equations is not achievable because to the presence of

thermal radiation, heat production, and varying thermal conductivity. Khan [45] the use of activation energy, thermal radiation, and applied magnetics force in nano-materials with advanced thermal properties allows for increased heat and mass transfer performance in numerous eras of engineering, industries, and technological processes. Energy generation from low-cost resources plays a renewable role in a country's economic development. With the use of thermally enhanced nanoparticles, this objective was successfully completed.

Furthermore, the bioconvection phenomena in nanomaterials lends itself to innovative biotech applications such as biosensors, enzymes, the petroleum industry, biofuels, and many others. The work aims to evaluate the rheological effects of Maxwell nanofluid together with swimming of gyrotactic microorganisms configured by a Riga surface due to such helpful uses of nano-particles and bio-convection phenomena. Khan [46] the goal of this research is to look at a three-dimensional rotating flow of water-based nanofluids that is caused by an endless rotating disc. The well-known Buongiorno model, which accounts for the combined impact of Brownian motion and thermophoresis, is used in the mathematical formulation. The condition of passively regulated wall nanoparticle volume fraction, which was recently proposed, was adopted.

Siddiqui [47] the current study proposes a permeable (suction/injection) chamber to manage the secondary vortices that form in the well-known lid-driven cavity flow using water-based ferrofluids. For the mathematical analysis of the physical problem, the Rosensweig model is useful. Turkyilmazoglu [48] The goal of this paper is to find exact solutions to the steady Navier–Stokes equations for incompressible Newtonian viscous fluid flow motion caused by a porous disc rotating at a constant angular speed. Analytical treatment of the three-dimensional equations of motion results in the derivation of accurate solutions, including suction and injection through the surface. The accurate velocity equations derived help to better understand the well-known thinning/thickening flow field impact of the suction/injection. Analytical formulae related to wall shear stresses are extracted using this solution. The energy equation is used to investigate the interaction of the resolved flow field with the surrounding temperature.

Turkyilmazoglu [49] the transparent impacts of the Buongiorno nanofluid model on the rate of heat and mass transfer in different fluid flow geometries are illustrated using a rigorous mathematical technique. Unlike the numerical simulations accessible in the recent open literature, the currently developed formulas allow us to analytically explain why the widely used Buongiorno nanofluid model accounting for Brownian motion and thermophoresis effects should promote or reduce heat and mass transmission. Two unique boundary restrictions are frequently taken into account in this model by active researchers working in this field. As a result, both the constant wall mass and the zero net particle mass flux on the wall are analytically analysed. Turkyilmazoglu [50] this research examines the impact of velocity slip and heat radiation on the magnetohydrodynamic hybrid Cu–Al2O3/water nanofluid flow across a permeable stretched sheet. To convert partial differential equations to ordinary differential equations, the similarity transformation is used. To answer the problem, an exact analytical procedure is used. The Maple application is used to make the calculations easier. The new added effects of velocity slip and heat radiation are taken into account in the model to examine the repercussions.

In this research work, mainly concentrating on Effects of thermophoresis, Brownian motion on temperature and concentration for boundary layer flow of a Casson nanofluid over a linearly stretched sheet. The local Nusselt and local Sherwood numbers have been compared primarily to variations in the Brownian Motion Parameter and the thermophoresis parameter. These findings are then tabulated and explained in detail in the results and discussion section and shown with the aid of graphs. The results revel that, there is an increase in temperature profile due to an increase in the values of Brownian motion parameter and the energy distribution increases with an increase in the values of Thermophoresis parameter.

Consequently, inspired by the previous research and use of the linear stretch sheet, we addressed the issue of the steady laminar 2D flow along with nanofluid sheat transfer from Casson through a permeable linearly stretching sheet as illustrated in Fig. 1.

## 2. Mathematical formulation

We assume that a viscous nanofluid flows through a flat stretching sheet to a laminar, incompressible, steady, 2*D* boundary layer corresponding to $y = 0$ plane, and then flow is constrained in $y$ more than 0. The flow is created via expanding the sheet with 2 equal and opposing forces in $x$-direction simultaneously. If the origin is constant, then the sheet is expanded at a speed $u_w(x) = ax$; an indicates "constant" and $x$ represents the coordinate obtained across the linear stretching plate.

The temperature $T$ and the percentage $C$ of nano particles at the stretching surface are considered to be constant $T_w$ and $C_w$. If $y$ tends to be infinite, the ambient temperature $T$ value and nano particles percentage $C$, are signified by $T_\infty$ & $C_\infty$. The suspended nano particles, as well as base fluid in thermal balancing, are examined.

The fundamental stable conservation of Cason nanofluids in terms of momentum, mass, nano particles, and thermal energy may be described in $X$ and $Y$ cartesian coordinates, see J. Buongiorno and R. U. Haq et al. [32,33]. In both instances, flow along with heat transfer properties of the linear stretching sheet is controlled by the following expressions under the boundary layer approximations.

$$\frac{\partial u}{\partial x} + \frac{\partial v}{\partial y} = 0, \tag{1}$$

$$u\frac{\partial u}{\partial x} + v\frac{\partial v}{\partial y} = v\left(1 + \frac{1}{\beta}\right)\frac{\partial^2 u}{\partial y^2}, \tag{2}$$

$$u\frac{\partial T}{\partial x} + v\frac{\partial T}{\partial y} = \alpha\left(\frac{\partial^2 T}{\partial y^2}\right) + \tau\left\{D_B\left(\frac{\partial C}{\partial y}\frac{\partial T}{\partial y}\right) + \left(\frac{D_T}{T_\infty}\right)\left[\left(\frac{\partial T}{\partial y}\right)^2\right]\right\}, \tag{3}$$

$$u\frac{\partial C}{\partial x} + v\frac{\partial C}{\partial y} = D_B\left(\frac{\partial^2 C}{\partial y^2}\right) + \left(\frac{D_T}{T_\infty}\right)\left(\frac{\partial^2 T}{\partial y^2}\right). \tag{4}$$

The boundary conditions are

$$v = -v_w, u = u_w(x), T = T_w, C = C_w, \quad \text{at} \quad y = 0. \tag{5}$$

$$u = v = 0, T = T_\infty, C = C_\infty, \quad \text{as} \quad y \to \infty. \tag{6}$$

Here $u$ & $v$ indicates the velocity components w.r.t $x$ and $y$-axis, $v$ =

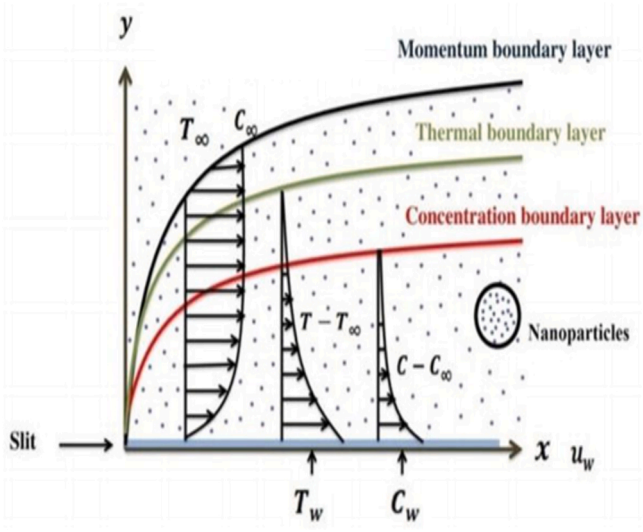


**Fig. 1.** Schematic representation of Physical problem.

$\mu/\rho_f$ denotes "kinematic viscosity", $\alpha = \kappa/(c\rho)_f$ signifies the "thermal diffusivity", $D_B$ represent the "Brownian diffusion coefficient", $D_T$ indicates the "diffusion coefficient" for thermophoresis, and $\tau = (\rho a)_P/(\rho a)_T$ signifies the relation in nano particle material's effective heat capacity and nanofluid heat capacity, $\beta$ denotes Casson fluid parameter, $T$ signifies the boundary layer temperature, $T_\infty$ signifies the ambient temperature. Here $u_w(x) = ax$ denotes the stretching sheet velocity, $T_w = T_\infty + b(x/1)^2$ signifies the stretching plate temperature, $C_w = C_\infty + c(x/1)^2$ denotes "nanoparticles volume fraction" over the surface. We are engaged in the aforementioned BVP solution and thus suggest the following transformations of similarity.

$$\eta = \left(\frac{a}{\upsilon}\right)^{1/2} y, \psi = (a\upsilon)^{1/2} x f(\eta), \theta(\eta) = \frac{T - T_\infty}{T_w - T_\infty}, \varphi(\eta) = \frac{C - C_\infty}{C_w - C_\infty}.$$

$$u = axf'(\eta), v = -\left(\frac{a\mu}{\rho}\right)^{\frac{1}{2}} f(\eta). \tag{7}$$

In Equation (7), $f$ signifies the dimension less stream function, the prime indicates difference w.r.t $\eta$ and $\psi$ indicates "stream function" and characterized as $u = \partial\psi/\partial y$, $v = -\partial\psi/\partial x$. Using transformations eq. (7) in eq. (1), we may accomplish continuity equation (incompressibility condition) is identically fulfilled and equations governing (2)–(4) have the form of non-linear ODEs:

$$\left(1 + \frac{1}{\beta}\right) f''' + ff'' - f'^2 = 0, \tag{8}$$

$$\theta'' + Prf' + PrNb\varphi'\theta' + PrNt\theta'^2 = 0, \tag{9}$$

$$\varphi'' + Lef\varphi' + \frac{Nt}{Nb}\theta' = 0. \tag{10}$$

Similarly, set of boundary conditions are expressed as,

$$f(0) = f_w, f'(0) = 1, \theta(0) = 1, \varphi(0) = 1 \quad \text{at} \quad \eta = 0,$$

$$f'(\infty) = 0, \theta(\infty) = 0, \varphi(\infty) = 0, \quad \text{as} \quad \eta \to \infty. \tag{11}$$

Here $\varphi$, $\theta$ and $f$ indicates nanoparticles concentration profiles, temperature, and dimensionless velocity. $\eta$ Indicates the similarity variable, the prime represents $\eta$ differentiation, and controlling factors seeming in equations (8)-(11) are expressed as

$$\left.\begin{aligned} Pr &= \frac{\upsilon}{\alpha} = 10 \to Pr \text{ and tl number}, \\ Le &= \frac{\upsilon}{D_B} = 10 \to Lew \text{ is number}, \\ Nb &= \frac{(\rho c)_p D_B (C_w - C_\infty)}{(\rho c)_f \upsilon}, (0.1 \le Nb \le 0.6) \to \text{Brownian motion parameter}, \\ Nt &= \frac{(\rho c)_p D_T (T_w - T_\infty)}{(\rho c)_f T_\infty \upsilon}, (0.1 \le Nt \le 0.6) \to \text{Thermophoresis parameter}, \\ f_w &= -\frac{v_w}{\sqrt{a\upsilon}}. \end{aligned}\right\} \tag{12}$$

The key physical parameters of relevance in present issue are the $Sh_x$ ("local Sherwood number"), $Nu_x$ ("local Nusselt number"), and $C_f$ ("local Skin friction coefficient") is expressed as

$$C_f = -\frac{\tau_w}{\rho u_w^2}, Nu_x = \frac{xq_w}{k(T_w - T_\infty)}, Sh_x = \frac{xq_m}{D_B(C_w - C_\infty)}. \tag{13}$$

where wall shear stress $\tau_w$, wall heat flux $q_w$, mass flux $q_m$ are given by:

$$\tau_w = \rho\upsilon\left(\frac{\partial u}{\partial y}\right)_{y=0}, q_w = -k\left(\frac{\partial T}{\partial y}\right)_{y=0}, q_m = -D_B.\left(\frac{\partial \varphi}{\partial y}\right)_{y=0} \tag{14}$$

## 3. Numerical solution of ODEs

Equations (8)–(10) corresponding boundary condition (11) are solved numerically by fourth order Runge-Kutta method with shooting technique. These equations are converted into a set of first order differential equations as follows:

$$\frac{df_0}{d\eta} = f_1,$$

$$\frac{df_1}{d\eta} = f_2,$$

$$\left(1 + \frac{1}{\beta}\right)\frac{df_2}{d\eta} = f_1^2 - f_0 f_2, \tag{15}$$

$$\frac{d\theta_0}{d\eta} = \theta_1,$$

$$\frac{d\theta_0}{d\eta} = -Pr(f_1 + Nb\varphi_1\theta_1 + Nt\theta_1^2), \tag{16}$$

$$\frac{d\theta_1}{d\eta} = -\left(Lef_0\varphi_1 + \frac{Nt}{Nb}\theta_1\right).$$

The associated boundary conditions take the form,

$$f_0(0) = f_w(0), f_1(0) = 1, \theta_0(0) = 1, \varphi_0(0) = 1,$$

$$f_1(\infty) = 0, \theta_0(\infty) = 0, \varphi_0(\infty) = 0.$$

An effective 4th order "Runge-Kutta" approach and the Shooting method were applied to examine the flow model from the above mentioned coupled ODEs (8)–(10) for various values of controlling factors like *Nt*, *Nb*, *Le*, *Pr*, and $\beta$. The ODEs are first broken up into a set of $1^s t$ ODEs. The coupled ODEs (8) and (10) are 2nd order in & and 3rd order in $f$ which were decreased to seven simultaneous eq. for 7 unknowns. To numerically resolve the equation system via the "Runge-Kutta" technique, the solution needs 7 initial conditions, however, 2 initial conditions are recognized in $f$ along with one initial condition all of $\varphi$ and $\theta$. Nevertheless, the values of $\varphi$, $\theta$ and fare given at $\eta \to \infty$. These constraints are used by the shooting technique to create unknown initial conditions $\eta = 0$. The key step in this approach is to take proper finite values $\eta_\infty$. Therefore, to calculate the $\eta_\infty$ value with the aid of a certain initial value and resolve the BVP containing Equations (8) and (10) to get $f''(0)$, $\theta'(0)$ and $\varphi'(0)$.

The solution procedure is continued with an additional bigger value $\eta_\infty$ till 2 consecutive values of $f''(0)$, $\theta'(0)$ and $\varphi'(0)$ differ merely after the required substantial digit. The final $\eta_\infty$ value is regarded as the limit for finite value $\eta_\infty$ for the specific collection of physical variables for measuring concentration, temperature along velocity are $f''(0)$, $\theta'(0)$ and $\varphi'(0)$ in the boundary layer. After, starting conditions we resolve this simultaneous equation system employing the 4th order "Runge-Kutta Integration" method. The $\eta_\infty$ is chosen between range 5–20 based on physical variables controlling the fluid flow to avoid numerical oscillation.

This research first converts the BVP into an IVP: "Initial Value Problem". This is addressed by properly estimating the missing initial value applying the shooting technique for multiple parameter combinations. The size of step $h = 0.1$ is utilized for computation applications. The error tolerance is also utilized. The findings are expressed via graphs and tables, and the major characteristics of the issues are addressed and evaluated.

## 4. Results and discussion

The mathematical model for concentration and temperature profiles for various parameter values are found. The findings are shown via

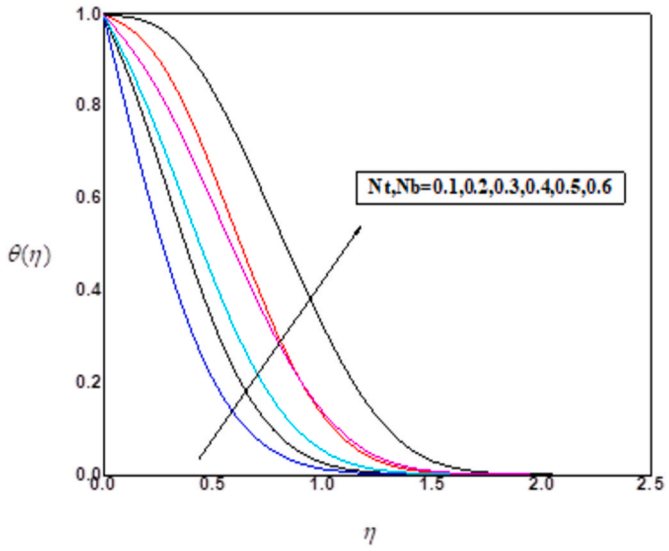


**Fig. 2.** Nb & Nt effects on temperature profiles for Pr = *Le* = 10 values.

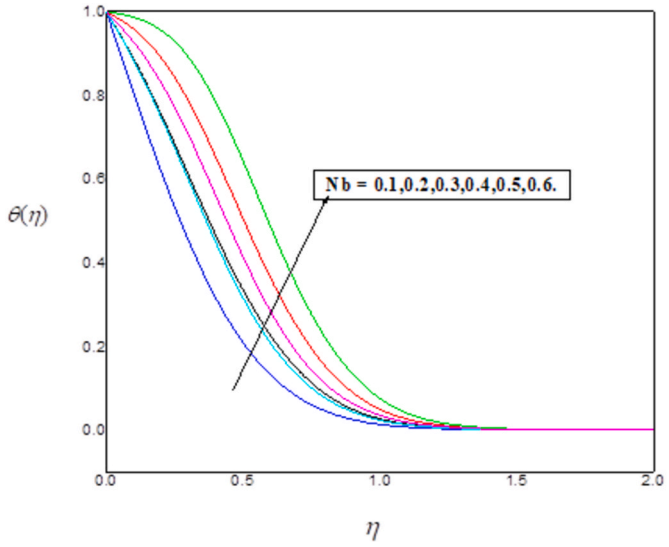


**Fig. 3.** Nb effects on temperature profiles for Pr = *Le* = 10,Nt = 0.1 values.

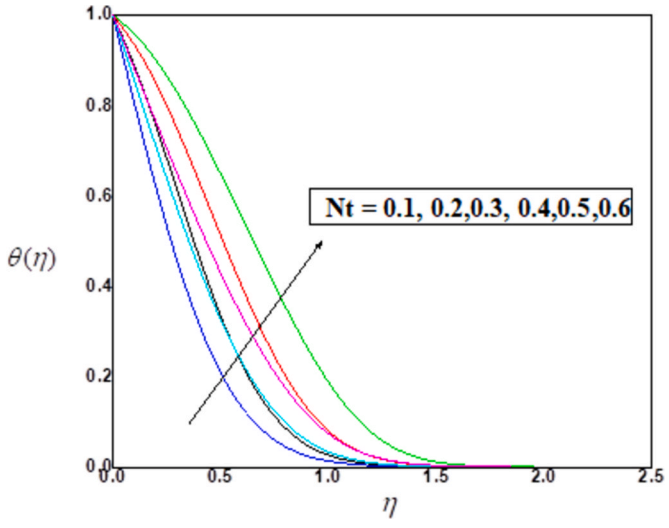


**Fig. 4.** Nt effects on temperature profiles for Pr = *Le* = 10,Nb = 0.1 values.

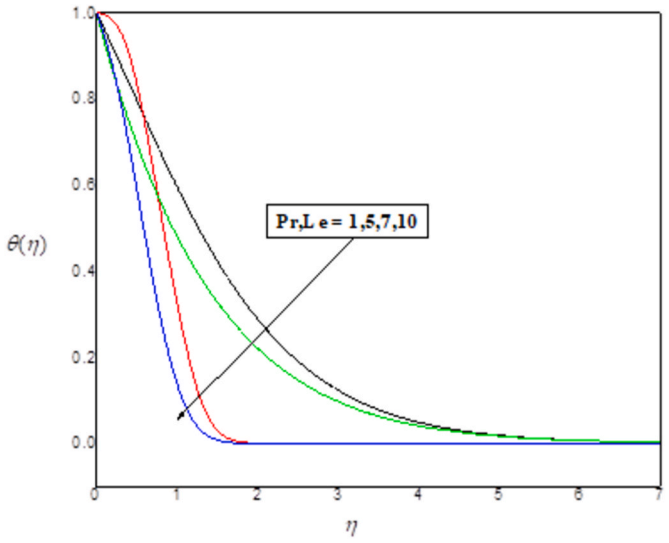


**Fig. 5.** *Le* and Prefects on temperature profiles for Nb = 0.5 and Nt = 0.5 values.

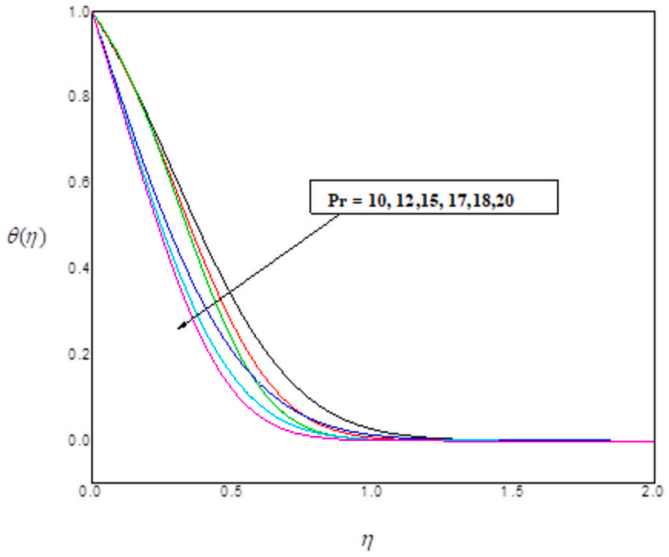


**Fig. 6.** Prefects on temperature profiles for Nb = 0.1, *Le* = 10, Nt = 0.1 values.

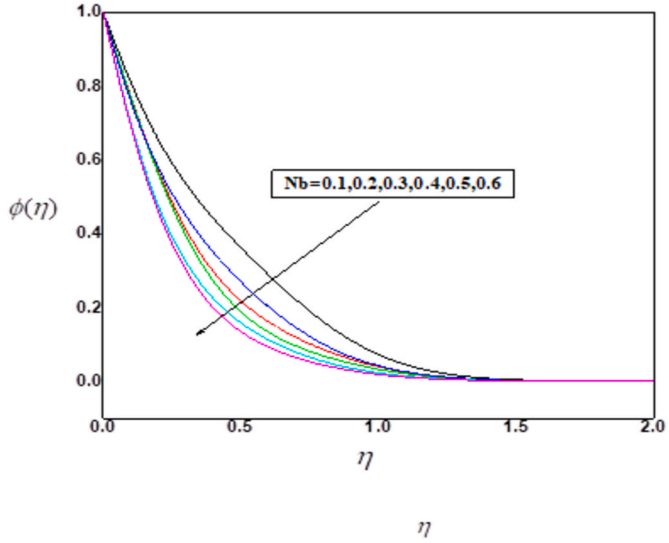


**Fig. 7.** Nb effects on concentration profiles for Nt = 0.1,*Le* = Pr = 10 values.

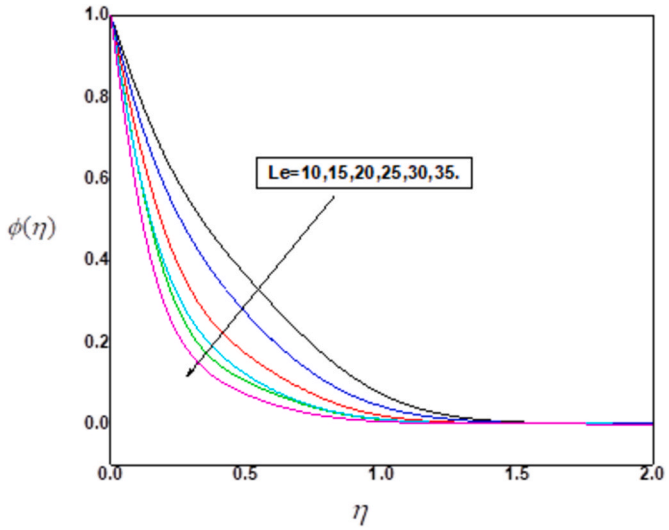


**Fig. 8.** *Le* effects on concentration profiles for Pr = 10,Nb=Nt = 0.1 values.

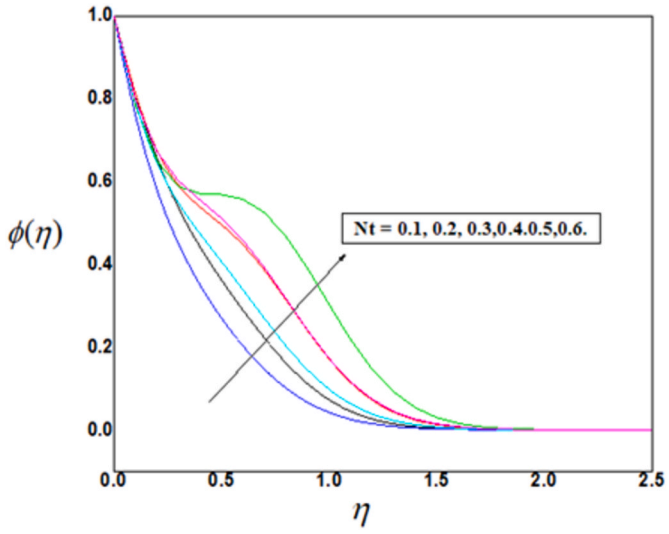


**Fig. 9.** Nt effects on concentration profiles for Pr = *Le* = 10,Nb = 0.1 values.

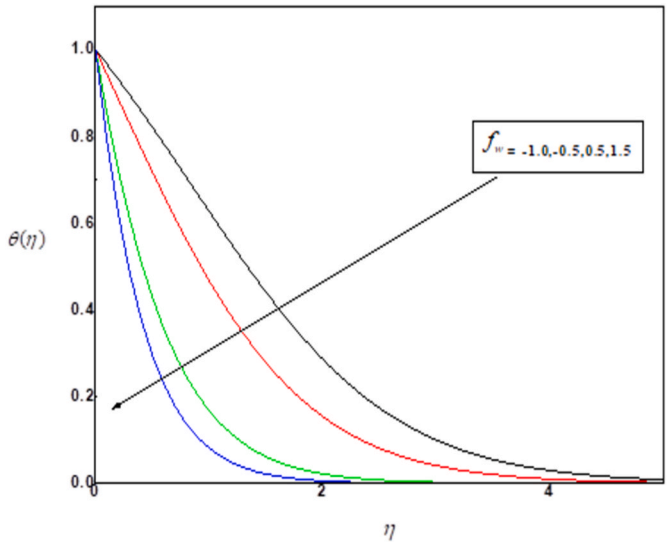


**Fig. 10.** Injection-suction parameter ($f_w$) effects on temperature profiles for Nt = 0.5,*Le* = 1.0,Nb = 0.5 Pr = 6.0 and $\beta$ = 5.0 values.

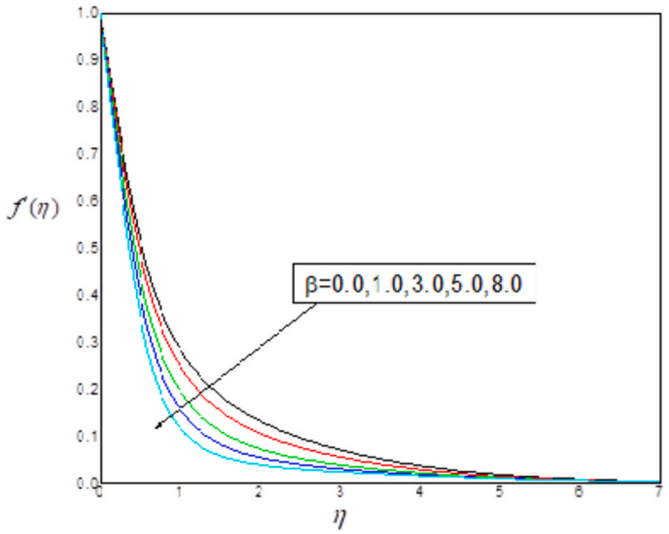


**Fig. 11.** Injection-suction parameter ($f_w$) effects on velocity profiles for Pr = 6.0, Nt = 0.5 *Le* = 1.0, Nb = 0.5, and $\beta$ = 5.0 values.

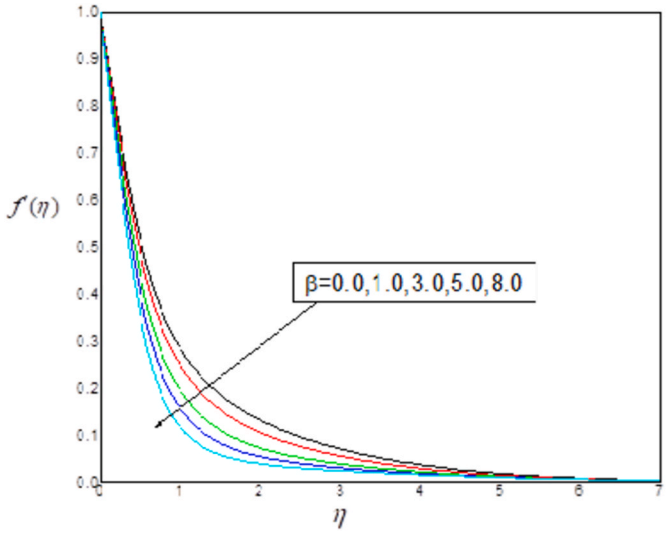


**Fig. 12.** Casson fluid parameter ($\beta$) effect on velocity profiles for $f_w$ = 0.5, Pr = 6.0, Nt = Nb = 0.5, *Le* = 1.0 values.

graphs Figs. 2–9, for the concentration and temperature profiles.

Figs. 2–4 illustrate the impacts of the parameters Nb & Nt for the values of the integers Pr & *Le*. The temperature function $\eta_\infty$ is anticipated to have the same shape as for a normal fluid. It is reported that the temperature rises as Nt as well as Nb rise based on the thickening of the thermal boundary layer fluid thickness. The effects of parameters Pr which correlates momentum transport and thermal transport properties of a fluid and Lewhich is the correlation the mass diffusion and the thermal conductivity of a fluid on the temperature profiles for the chosen values ofthe parameter Nt and Nb are shown in Figs. 5 and 6. It is reported that the temperature drops with growing Pr and *Le* led to thinning boundary layer fluid thickness. An increase in these parameters gradually allows fluid to expel the heat from the fluid to the external environment or adjacent body which leads to a decrease in the temperature of the fluid.

Figs. 7–9 demonstrate the effects of Nb, *Le* and Nt on concentration profiles of the chosen values of the parameters which results the thickening of the nanofluids boundary concentration layer. The Brownian motion is shown the reverse behaviour on the nano fluids concentration

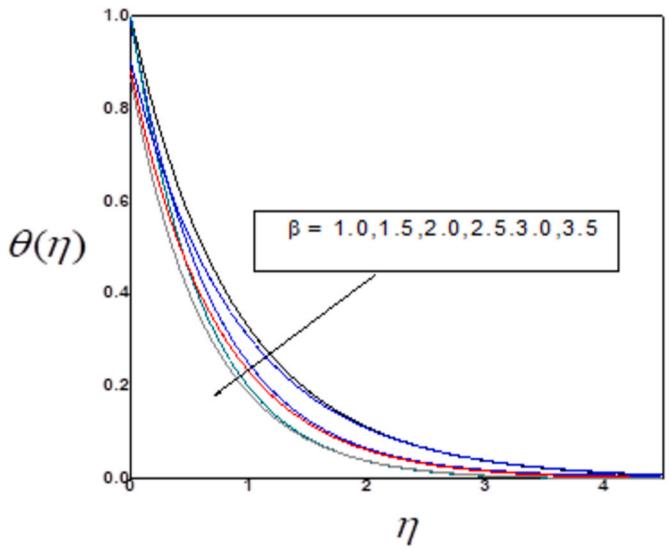


**Fig. 13.** Casson fluid parameter ($\beta$) effect on temperature profiles for $f_w = 5.0$, Pr = 6.0, Nt = Nb = 0.5, $Le = 1.0$ values.

boundary layer. It is observed that both friction factor coefficients increase with an increase in nanoparticle volume fraction, while an opposite phenomenon can observe in the case of the Sherwood number. Hence the concentration reduces with an increase in the value of Nb. Observation shows that Nt will be affecting the increasing nanofluids concentration with higher values of the chosen parameter.

In Fig. 10. Indicates profile of temperature on the thermal boundary layer enhances with the enhancement of $f_w$.

Fig. 11 the consequence of the Injection/suction parameter (fw)on the velocity profile and is found here, that it results in the decelerating velocity boundary layer thickness. It seems like a rise in the fluid viscosity also reduces the boundary layer thickness owing to yield stress.

Fig. 12 depicts the impact of $f_w$ which results in reducing velocity inside the boundary layer. It is also noticed that velocity reduces due to suction whereas it increases with injection.

In Fig. 13 influences the effects of Casson fluid parameter ($\beta$) to improve the temperature inside the boundary layer due to which, a reduction in the yield stress occurs. Casson fluid is treated as fluid with variable plastic dynamic viscosity with a strong effect of yield stress, the velocity increases near the wall and negligibly decreases far from the vertical heated wall for an increase in the values of Casson fluid parameter ($\beta$).

Finally, a comparison was made with publications in the literature to verify the precision of the current findings. Table 1 summarizes the findings for local Sherwood as well as local "Nusselt number" with Nt ("Thermophoresis Parameter") & Nb ("Brownian Motion Parameter")for $Le = \Pr = 10$ found in the current study, which is in close line with the findings noted by Pop and Khan [15] and Aminreza Noghrehabad [20].

## 5. Conclusion

1. There is increment in temperature profile for increasing values of Brownian motion parameter.
2. Reduction in concentration profiles is noticed with the growing values of Brownian motion parameter and thermophoresis parameter intensify the concentration profiles.
3. The energy distribution grows with increment in the values of Thermophoresis parameter.
4. It is observed that the Nusselt number decreases by enhancing the Prandtl number, Thermophoresis parameter and Brownian motion parameter
5. The temperature intensifies with increasing values of Thermophoresis parameter and Brownian motion parameter. While a reverse behaviour is found to be true with the increasing values of Prandtl number.

## Credit author statement

Jagadish V Tawade: Conceptualization; Data curation; Formal analysis; Investigation; Methodology; Resources; Software; Validation; Visualization; Roles/Writing – original draft; Writing – review & editing. C. N. Guled: Conceptualization; Data curation; Formal analysis; Investigation; Methodology; Resources; Software; Validation; Writing – original draft; Writing – review & editing. Samad Noeiaghdam: Formal analysis; Funding acquisition; Investigation; Methodology; Project administration; Resources; Supervision; Writing – review & editing. Unai Fernandez-Gamiz: Formal analysis; Funding acquisition; Investigation; Methodology; Project administration; Resources; Software; Validation; Writing – review & editing. Vediyappan Govindan: Conceptualization; Formal analysis; Methodology; Resources; Software; Validation; Visualization; Writing – review & editing. Sundrappan Balamuralitharan: Conceptualization; Data curation; Formal analysis; Software; Supervision; Validation; Writing – review & editing.

## Availability of data and material

All data that support the findings of this study are included within the article (and any supplementary files).

## Funding

The work of U.F.-G. was supported by the government of the Basque Country for the ELKARTEK21/10 KK-2021/00014 and ELKARTEK22/85 research programs, respectively.

**Table 1**
Findings comparison for the local Nusselt & local Sherwood number when $\Pr = Le = 10$, $fw = \beta = 0$.

| | | Pop and khan [15] | Aminreza Noghrehabad [16] | Current finding | Pop and Khan [15] | Aminreza Noghrehabad [16] | Current finding |
|---|---|---|---|---|---|---|---|
| Nt | Nb | $-\theta'(0)$ | $-\theta'(0)$ | $-\theta'(0)$ | $-\theta'(0)$ | $-\theta'(0)$ | $-\theta'(0)$ |
| 0.1 | 0.1 | 2.1294 | 2.1293938 | 2.129346 | 0.9524 | 0.9523768 | 0.952398 |
| 0.2 | 0.1 | 2.2740 | 2.2740215 | 2.273857 | 0.6932 | 0.6931743 | 0.693215 |
| 0.3 | 0.1 | 2.5286 | 2.5286382 | 2.528362 | 0.5201 | 0.5200790 | 0.520130 |
| 0.4 | 0.1 | 2.7952 | 2.7951701 | 2.794799 | 0.4026 | 0.4025808 | 0.402636 |
| 0.5 | 0.1 | 3.0351 | 3.0351425 | 3.034698 | 0.3211 | 0.3210543 | 0.321110 |
| 0.1 | 0.2 | 2.3819 | 2.3818706 | 2.381470 | 0.5056 | 0.5055814 | 0.505589 |
| 0.1 | 0.3 | 2.4100 | 2.4100188 | 2.409953 | 0.2522 | 0.2521560 | 0.252444 |
| 0.1 | 0.4 | 2.3997 | 2.3996502 | 2.399450 | 0.1194 | 0.1194059 | 0.119402 |
| 0.1 | 0.5 | 2.3836 | 2.3835712 | 2.383571 | 0.0543 | 0.0542534 | 0.054253 |
| 0.2 | 0.3 | – | – | 2.514821 | – | – | 0.181881 |
| 0.3 | – | – | – | 2.608559 | – | – | 0.135775 |

## Declaration of competing interest

The authors declare that they have no known competing financial interests or personal relationships that could have appeared to influence the work reported in this paper.

## Nomenclature

| | |
|---|---|
| $T$ | fluid temperature within the boundary layer |
| $\beta$ | Casson fluid parameter |
| $u$, $v$ | velocity component w. r.$tx\&y$-axis |
| $Pr$ | Pr and $t_l$ number |
| $p$ | the fluid pressure |
| $Nb$ | Brownian motion parameter |
| $Le$ | Lewis numbers |
| $Nt$ | thermophores is parameter |
| $Nu_x(nur)$ | Local Nusselt number |
| $a$, $b$, $c$ | constant |
| $C_w$ | nano particles volume fraction on a stretching surface |
| $Sh_x(Shr)$ | local Sherwood number |
| $f(\eta)$ | dimensionless stream function |
| $\mathrm{Re}_x$ | local Reynolds number |
| $u_w$ | stretching sheet velocity |
| $D_r$ | thermophoresis diffusion coefficient |
| $T_w$ | uniform temperature across the sheet surface |
| $D_B$ | Brownian diffusion coefficient |
| $C_\infty$ | the ambient nano particles volume fraction |
| $T_\infty$ | ambient temperature far away from the sheet surface |
| $\kappa$ | thermal conductivity |
| $c_f$ | skin friction coefficient |

*Greek symbols*

| | |
|---|---|
| $(a\rho)_f$ | heat capacity of the fluid |
| $\psi$ | stream function |
| $(a\rho)_P$ | effective heat capacity of a nanofluid |
| $\alpha$ | thermal diffusivity |
| $\rho_f$ | fluid density |
| $\upsilon$ | kinematic fluid viscosity |
| $\tau$ | parameter characterized by $(a\rho)_P/(a\rho)_f$ |
| $\theta$ | dimensionless temperature |
| $\mu$ | dynamic fluid viscosity |
| $\eta$ | dimensionless similarity variable |
| $\varphi$ | dimensionless concentration function |

*Subscripts*

| | |
|---|---|
| $w$ | surface condition |
| $\infty$ | free stream condition |

## References


[1] B.C. Sakiadis, Boundary layer behavior on a continuous solid surface: boundary layer equations for two dimensional and axisymmetric flow, AIChE J. 7 (1961) 26–28.

[2] I.C. Liu, Flow and heat transfer of an electrically conducting fluid of second grade over a stretching sheet subject to a transverse magnetic field, Int. J. Heat Mass Tran. 47 (2004) 4427–4437.

[3] S.K. Khan, M. Subhas Abel, M. South Ravi, Viscoelastic M.H.D. flow heat and mass transfer over a porou stretching sheet with the dissipation of energy and stress work, Int. J. Heat Mass Tran. 40 (2003) 47–57.

[4] R. Cortell, Effects of viscous dissipation and work done by deformation on the MHD flow and heat transfer of a viscoelastic fluid over a stretching sheet, Phys. Lett. 357 (2006) 298–305.

[5] B.S. Dandapat, B. Santra, K. Vajravelu, The effects of variable fluid properties and thermocapillary on the flow of a thin film on an unsteady stretching sheet, Int. J. Heat Mass Tran. 50 (2007) 991–996.

[6] S. Nadeem, A. Hussain, M. Khan, HAM solutions for boundary layer flow in the region of the stagnation point towards a stretching sheet, Commun. Nonlinear Sci. Numer. Simulat. 15 (2010) 475–481.

[7] N. Bachok, A. Ishak, Flow and heat transfer over a stretching cylinder with prescribed surface heat flux Malays, J. Math. Sci. 4 (2010) 159–169.

[8] N. Bachok, A. Ishak R. Nazar, Flow and heat transfer over an unsteady stretching sheet in a micropolar fluid with prescribed surface heat flux, Int. J. Math. Mod. Meth. Appl. Sci. (2010) 167–176.

[9] N. Bachok, A. Ishak, I. Pop, On the stagnation point flow towards a stretching sheet with homogeneous-heterogeneous reactions effects, Commun. Nonlinear Sci. Numer. Simulat. 16 (2011) 4296–4302.

[10] N. Bachok, A. Ishak, R. Nazar, Flow and heat transfer over an unsteady stretching sheet in a micropolar fluid, Meccanica 46 (2011) 935–942.

[11] A.V. Kuznetsov, D.A. Nield, The natural convective boundary-layer flow of a nanofluid past a vertical plate, Int. J. Therm. Sci. 47 (2010) 243–247.

[12] W. Ibrahim, ShankerB, Boundary layer flow and heat transfer of a nanofluid over a vertical plate with convective surface boundary condition, J Fluid Eng-Trans ASME 134 (2012) 81203–81212.

[13] AzizA. MakindeOD, Boundary layer of a nanofluid past a stretching sheet with convective boundary condition, Int. J. Therm. Sci. 50 (2011) 1326–1332.

[14] M. Mostafa, PopI. HayatT, AsgharS, ObaidatS, Stagnation point flow of a nanofluid towards a stretching sheet, Int. J. Heat Mass Tran. 54 (2011) 5588–5594.

[15] W.A. Khan, PopI, Boundary layer flow of a nanofluid past a stretching sheet, Int. J. Heat Mass Tran. 53 (2010) 2477–2483.

[16] S. Arulmozhi, K. Sukkiramathi, S.S. Santra, R. Edwan, U. Fernandez-Gamiz, S. Noeiaghdam, Heat and Mass transfer analysis of Radiative and Chemical reactive effects on MHD Nanofluid over an infinite moving vertical plate, Results Eng. 14 (2022) 100394, https://doi.org/10.1016/j.rineng.2022.100394.

[17] M.S. Khan, S. Mei, Shabnam, U. Fernandez-Gamiz, S. Noeiaghdam, A. Khan, S. A. Shah, Electroviscous effect of water-base nanofluid flow between two parallel disks with suction/injection effect, Mathematics 10 (2022) 956, https://doi.org/10.3390/math10060956.

[18] M.S. Khan, S. Mei, Shabnam, U. Fernandez-Gamiz, S. Noeiaghdam, A. Khan, Numerical simulation of a time-dependent electroviscous and hybrid nanofluid with Darcy-Forchheimer effect between squeezing plates, Nanomaterials 12 (2022) 876, https://doi.org/10.3390/nano12050876.

[19] M.S. Khan, S. Mei, Shabnam, U. Fernandez-Gamiz, S. Noeiaghdam, S.A. Shah, A. Khan, Numerical analysis of unsteady hybrid nanofluid flow comprising CNTs-Ferrousoxide/water with variable magnetic field, Nanomaterials 12 (2022) 180, https://doi.org/10.3390/nano12020180.

[20] A. Noghrehabadi, R. Pourrajab, M. Ghalambaz, Effect of partial slip boundary condition on the flow and heat transfer of nanofluids past stretching sheet prescribed constant wall temperature, Int. J. Therm. Sci. 54 (2012) 253–261.

[21] W. Ibrahim, B. Shankar, MHD boundary layer flow and heat transfer of a nanofluid past a permeable stretching sheet with velocity, thermal and solutal slip boundary conditions, Comp. Fluids75 (2013) 1–10.

[22] E. Magyari, B. Keller, Heat and mass transfer in the boundary layers on an exponentially stretching continuous surface, J. Phys. D Appl. Phys. 32 (1999) 577–585.

[23] B. Bidin, R. Nazar, Numerical solution of boundary layer flow over an exponentially stretching sheet with thermal radiation, Eur. J. Sci. Res. 33 (2009) 710–717.

[24] A. Ishak, MHD boundary layer flow due to an exponentially stretching sheet with radiation effect, Sains Malays. 40 (2011) 391–395.

[25] S. Nadeem, T. Hayat, M.Y. Malik, S.A. Rajput, Thermal radiations effects on the flow by an exponentially stretching surface, a series solution 65 (2010) 301–309.

[26] S. Nadeem, S. Zaheer, T. Fang, Effects of thermal radiations on the boundary layer flow of Jeffrey, fluid over an exponentially stretching surface 57 (2011) 187–205.

[27] E.M.A. Elbashbeshy, Heat transfer over an exponentially stretching continuous surface with suction, Arch. Mech. 53 (2001) 643–651.

[28] S.K. Khan, Sanjayanand, Viscoelastic boundary layer flow and heat transfer over an exponentially stretching sheet, Int. J. Heat Mass Tran. 48 (2005) 1534–1542.

[29] V. Singh, Shweta Agarwal, Numerical study of heat transfer for two types of viscoelastic fluid over an exponentially stretching sheet with variable thermal conductivity and radiation in a porous medium, I, J. Therm. Sci. 77 (2012) 144–153.

[30] S. Nadeem, R. Mehmood, N.S. Akbar, Optimized analytical solution for the oblique flow of a Casson-nano fluid with convective boundary conditions, Int. J. Therm. Sci. 78 (2014) 90–100.

[31] M.H. Abolbashari, N. Freidoonimehr, F. Nazari, M.M. Rashidi, Analytical modeling of entropy generation for Casson nano-fluid flow induced by a stretching surface, Adv. Powder. Tech 26 (2015) 542–552, 2015.

[32] J. Buongiorno, Convective transport in nanofluids, J. Heat Trans. 128 (3) (2006) 240–250.

[33] R.U. Haq, S. Nadeem, Z.H. Khan, T.G. Okedayo, Convective heat transfer and MHD effects on Casson nanofluid flow over a shrinking sheet, Central, Eur. J. Phys. 12 (2014) 862–871.

[34] Sk R.E. Rabbi, Md S. Khan, S.M. Arifuzzaman, S. Islam, P. Biswas, B.M.J. Rana, A. Mamun, T. Hayat, S.F. Ahmmed, Numerical simulation of a non-linear nanofluidic model to characterise the MHD chemically reactive flow past an inclined stretching surface, Partial Differ. Equ. Appl. Math. 5 (2022) 100332. ISSN2666-8181.

[35] B.M.J. Rana, S.M. Arifuzzaman, S. Islam, Sk R.E. Rabbi, A. Mamun, M. Mazumder, K.C. Roy, Md S. Khan, Swimming of microbes in blood flow of nano-bioconvective Williamson fluid, Therm. Sci. Eng. Prog. 25 (2021) 101018. ISSN 2451-9049.

[36] B.M.J. Rana, S.M. Arifuzzaman, S. Islam, Sk R.E. Rabbi, S.F. Ahmed, S. Khan, Energy and magneticflow analysis of Williamson micropolar nanofluid through stretching sheet, Int. J. Heat Technol. 37 (2) (2019) 487–496, https://doi.org/10.18280/ijht.370215.

[37] S.M. Arifuzzaman, M.S. Khan, M.F.U. Mehedi, B.M.J. Rana, S.F. Ahmmed, Chemically reactive and naturally convective high speed MHD fluid flow through

an oscillatory vertical porous plate with heat and radiation absorption effect, Eng. Science and Technology, an International Journal 21 (Issue 2) (2018) 215–228. ISSN 2215-0986.

[38] A. Mamun, A. Arifuzzaman, Sk R.E. Rabbi, Numerical simulation of periodic MHD casson nanofluid flow through porous stretching sheet, SN Appl. Sci. 3 (2021) 271, https://doi.org/10.1007/s42452-021-04140-3.

[39] M.I. Khan, F. Alzahrani, Entropy-optimized dissipative flow of Carreau–Yasuda fluid with radiative heat flux and chemical reaction, Eur. Phys. J. Plus 135 (2020) 516, https://doi.org/10.1140/epjp/s13360-020-00532-3.

[40] C. Yuming, A. Samaira, M. Khan, S. Khan, M. Nazeer, I. Ahmad, I. Tlili, Nonlinear radiative bioconvection flow of Maxwell nanofluid configured by bidirectional oscillatory moving surface with heat generation phenomenon, Phys. Scripta 95 (2020) 105007, https://doi.org/10.1088/1402-4896/abb7a9.

[41] Y.M. Chu, M.I.U. Rehman, M.I. Khan, S. Nadeem, S. Kadry, Z. Abdelmalek, N. Abbas, Transportation of heat and mass transport in hydromagnetic stagnation point flow of Carreau nanomaterial: dual simulations through Runge-Kutta Fehlberg technique, Int. Commun. Heat Mass Tran. 118 (2020) 104858. ISSN 0735-1933.

[42] M.K. Nayak, S. Shaw, M.I. Khan, O.D. Makinde, Y.M. Chu, S.U. Khan, Interfacial layer and shape effects of modified Hamilton's Crosser model in entropy optimized Darcy-Forchheimer flow, Alex. Eng. J. 60 (Issue 4) (2021) 4067–4083. ISSN 1110-0168.

[43] M. Khan, Q. Sumaira, S. Faisal, R. Kumar, P.R.J. Gowda, B.C. Prasannakumara, C. Yuming, K. Seifedine, Marangoni convective flow of hybrid nanofluid (MnZnFe2O4-NiZnFe2O4-H2O) with Darcy Forchheimer medium, Ain Shams Eng. J. 12 (2021), https://doi.org/10.1016/j.asej.2021.01.028.

[44] Y.M. Chu, M. Nazeer, M.I. Khan, F. Hussain, H. Rafi, S. Qayyum, Z. Abdelmalek, Combined impacts of heat source/sink, radiative heat flux, temperature dependent thermal conductivity on forced convective Rabinowitsch fluid, Int. Commun. Heat Mass Tran. 120 (2021) 105011. ISSN 0735-1933.

[45] K. Ramesh, S.U. Khan, M. Jameel, M.I. Khan, Y.M. Chu, S. Kadry, Bioconvection assessment in Maxwell nanofluid configured by a Riga surface with nonlinear thermal radiation and activation energy, Surface. Interfac. 21 (2020) 100749. ISSN 2468-0230.

[46] J.A. Khan, M. Mustafa, T. Hayat, M. Turkyilmazoglu, A. Alsaedi, Numerical study of nanofluid flow and heat transfer over a rotating disk using Buongiorno's model, Int. J. Numer. Methods Heat Fluid Flow 27 (1) (2017) 221–234, https://doi.org/10.1108/HFF-08-2015-0328.

[47] A.A. Siddiqui, M. Turkyilmazoglu, A new theoretical approach of wall transpiration in the cavity flow of the ferrofluids, Micromachines 10 (2019) 373, https://doi.org/10.3390/mi10060373.

[48] M. Turkyilmazoglu, Exact solutions for the incompressible viscous fluid of a porous rotating disk flow, Int. J. Non Lin. Mech. 44 (4) (2009) 352–357.

[49] M. Turkyilmazoglu, On the transparent effects of Buongiorno nanofluid model on heat and mass transfer, Eur. Phys. J. Plus 136 (2021) 376.

[50] W.N. Syahirah, N. Arifin, M. Turkyilmazoglu, M. Hafidzuddin, N. Rahmin, MHD hybrid Cu-Al2O3/water nanofluid flow with thermal radiation and partial slip past a permeable stretching surface: analytical solution, J. Nano Res. 64 (2020) 75–91. https://dx.doi.org/10.4028/www.scientific.net/JNanoR.64.75.